# 行政院國家科學委員會專題研究計畫　期中進度報告

## 過共晶鋁矽合金粉末成形新方法之研究(2/3)

計畫類別：個別型計畫
計畫編號：NSC92-2216-E-009-004-
執行期間：92 年 08 月 01 日至 93 年 07 月 31 日
執行單位：國立交通大學材料科學工程研究所

計畫主持人：朝春光

報告類型：精簡報告

處理方式：本計畫可公開查詢

中　華　民　國 93 年 5 月 31 日

# Wear and strength properties of hypereutectic Al-Si alloys prepared by powder thixocasting

陳俊沐 [1,2]　楊智超 [2]　蘇健忠 [2]　朝春光 [1]
[1] 交通大學材料研究所　[2] 工業技術研究院材料所
（NSC91-2216-E-009-022）

Abstract

Powder thixocasting (PT) is a newly developed technique that combines powder processing and semi-solid forming to achieve net-shape forming the alloys with fine microstructure. This study attempts to reveal the wear performance of Al-25Si-2.5Cu-1Mg and Al-20Si-5Fe alloys prepared by this new technique. For comparison, LM13 and Al-25Si-2.5Cu-1Mg alloy prepared by conventional ingot metallurgy (IM) were also examined. Microstructure observation shows that the powder thixocast alloys exhibit much finer Si particulates than those produced using the IM routes. Dry sliding wear were conducted by using a pin-on-disc machine with contact load increasing stepwise until seizure occurs. Experimental results show Al-25Si-2.5Cu-1Mg (PT) alloy in T6-treated condition and under high load sliding conditions exhibits outstanding wear resistance. The superior wear performance of the alloy indicates the potential of powder thixocasting for fabricating high performance of hypereutectic Al-Si-X alloys.
*Keywords:* Aluminum-silicon; Wear; Thixocasting; Powder processing

## 1. INTRODUCTION

The high wear resistance, low thermal expansion, and reduced density make hypereutectic Al-Si alloys very attractive for the transport application [1]. Among the most common applications are components, such as cylinder liners, pistons, engine blocks, and compressor scrolls [1]. Most of these components are fabricated by liquidus casting routes owing to their complex shape. However, the castings always contain large primary Si particles even though modification of Si is used [2]. Since the large Si particles reduce tool life during machining and also greatly reduce material strength [3], refining the Si size has been attractive to many researchers. Although rapid solidification processes (RSPs) are recognized to be the most promising method in refining the Si sizes, they only produce ribbons (by melt spinning), powders (by gas-atomization), or preforms (by spray deposition). Therefore, additional PM processes such as powder forging [3] or extrusion [4] are required to produce the components. Nevertheless, the PM processes still exhibit the drawback for difficultly achieving net shape forming of the component.

Recently, the authors developed a new method introduced as powder thixocasting, that combines the powder process and thixocasting techniques for achieving net-shape forming of hypereutectic Al-Si components with integrity and with fine Si particles evenly distributed in matrix [5]. This work attempts to reveal the wear performance of hypereutectic Al-Si-X alloys fabricated by this new method.

## 2. EXPERIMENTAL

The chemical compositions of the alloys were shown in Table 1. Alloys Al-25SiCuMg (PT) and Al-20Si5Fe (PT) were produced using powder thixocasting, alloy Al-25SiCuMg (IT) were produced using conventional thixocasting, and finally alloy LM13 were cast in a permanent metallic mould. Thixocasting is a semi-solid metal forming process that produces net-shaped component using a die-casting machine and using a “non-dentritic” solid metal feedstock heated to a semi-solid state. In powder thixocasting of alloy Al-25SiCuMg (IT), the feedstock was prepared by powder process. Figure 1 schematically depicts the powder thixocasting processes. At first the Al-Si prealloyed powders were hot consolidated into powder preforms, which were then heated to a semisolid temperature by induction coils. Afterward, they were immediately transferred to a sleeve and extruded into a mould cavity by a plunger in a die-casting machine. The detail procedures were published elsewhere [5]. On the other hand, in conventional thixocasting the feedstock for thixocasting the Al-25SiCuMg (IT) alloy was prepared by squeeze casting of the alloy at 800°C and under 85Mpa and without any primary Si refiner used.

Sliding wear tests were performed at room temperature and for both as-thixocast and T6 treated samples. The T6 condition was 500°C for 4 hours followed by 175°C for 10 hours for the Al-25Si-2.5Cu-1Mg alloys, while it was 520°C for 4 hours followed by 175°C for 8 hours for LM13 alloys. Wear tests were conducted using a conventional pin-on-disc testing machine. The pins, of 8 mm in diameter and 15 mm in length, were machined from the Al-Si alloys. Disc-shaped counter material was BS 708 M40 steel with hardness being adjusted by heat-treatment to be Rockwell C 40. All tests were conducted under no lubricant condition and at room temperature. The applied wear load was increased stepwise during wearing tests until the onset of specimen seizure was noted. The specimen seizure was indicated in term of abnormal noise in the pin-disc assembly and large adhesion of the specimen material to the disc. For each wearing step, the pin was slid at a constant speed of 1.57 m s-1 for a distance of 1.88 km under a constant load. At the end of each the step, the rotation of the steel disc was stopped automatically and a surface thermal couple was immediately used to touch the worn surface of the pin to measure the bulk temperature of the pin. Afterward, the worn pin was withdrawn from the fixture of wear machine and was weighed to obtain the wear rate. After interval of about 5 minutes, the same pin that had been worn and weighed was used again in next step for wearing test. The wear rate values were calculated from the weight loss measurements and expressed in terms of volume loss per unit sliding distance ($m^3/m$). Each wear rate value was averaged from data obtained at least on two different wearing pins.

## 3. RESULTS AND DISCUSSION

### *3.1 Microstructure*

Optical micrographs investigation shows that fine

and equiaxed particulates of primary Si phase are uniformly embedded in a matrix of Al-25SiCuMg powder (Fig.2a). The matrix is composed mostly of α-Al grains and eutectic Si particulates, which may be considered to be similar with the Al-12wt%Si eutectic formed under equilibrium conditions. A small amount of $CuAl_2$ and $Al_5Cu_2Mg_8Si_6$ ('Q' [6,7]) may also exist in this matrix. Comparing with the Al-25SiCuMg powder, the Al-20SiFe powders also possesses long needle-shaped and iron-rich particulates having size of 20-80 μm, embedded in the Al-12%Si matrix (Fig.2b). A black network is found in the matrix of Al-25SiCuMg powder, whereas no sign of the network is found in Al-20SiFe powder. The black network should consist of the eutectic Si and $CuAl_2$, which crystallize at α-Al grain boundaries.

After thixocasting, some interesting transformations of the microstructures can be noted. Firstly, Fig.3a clearly shows that primary Si particulates of Al-25SiCuMg alloy have a tendency to cluster together. However, this clustering seems to be hampered by the rod-shaped intermetallic in Al-20SiFe alloy (Fig.3b). Secondarily, the long needle-shaped intermetallic phases in the Al-20SiFe powder (Fig.2b) transformed to rectangular shape (Fig.3b). According to our X-ray diffraction investigation, the needlelike phases is verified to be composed most of metastable δ -$Al_4FeSi_2$ of tetragonal crystal structure, whereas the rectangular phase is the equilibrium β - $Al_5SiFe$. The formation of non-equilibrium δ -$Al_4Si_2Fe$ phase indicates that the powders undergo extensive undercooling, prior to solidification [8-10]. However, our results indicates that after thixocasting the metastable δ -$Al_4Si_2Fe$ phase transformed to equilibrium β - $Al_5SiFe$ phase. It is suggested that the phase transformation of the δ -$Al_4Si_2Fe$ particulates into β - $Al_5SiFe$ phase together with the grain growth simultaneously occurred when a semisolid powder slurry was heated and deformed to fill a mold cavity.

After thixocasting, it is worthy to note that the eutectic Si particulars in the matrix of Al-20SiFe alloy (Fig.3b) are much coarser than that of Al-25SiCuMg (Fig.3a). This coarser eutectic matrix microstructure may indicate that the eutectic Al-12%Si matrix in Al-20SiFe powder could once melted, leading to high liquid fraction after heating to semisolid state. Since the coarser microstructure of eutectic matrix may indicate that the eutectic Al-Si melt was solidified at a low cooling rate.

The high liquid volume in the Al-20SiFe powder compacts during semisolid processing causes many detrimental effects. Firstly, it causes the Al-20SiFe alloy (Fig.3b) have larger primary Si than that in Al-20SiCuMg alloy (Fig.3a). The primary Si size in both powders is 3-9 μm, whereas after thixocasting it becomes 5-13 μm and 8-25 μm in Al-25SiCuMg and Al-20SiFe, respectively. In our previous study [5], we found that the coarsening behavior of primary Si particulates could be retarded by stabilization of solid α-Al grains in the semisolid slurry. This is because that the solid α-Al grains in the slurry are considered can prevent primary Si particulates from contacting with the melt, leading to low diffusion behavior and consequent to low Si grain growth. Since the Al-12%Si matrix of Al-20SiFe powder was almost liquefied, high fraction of liquid occurs and α-Al grains could hardly be stabilized in semisolid state. As a result, primary Si particulate size in Al-20SiFe alloy becomes larger after thixocasting compared with Al-25SiCuMg alloy.

Figure 4a shows a typical optical microstructure of Al-5SiCuMg alloy fabricated using conventional liquidus casting method. After thixocasting, microstructure refinement in Al-12%Si matrix can be noted. However, the thixocast alloy still shows drastically large primarily Si particulates even with maximum size up to 500 μm (Fig.4b).

*3.2 Tensile properties and microhardness*

Table 2 presents strength and hardness values of the Al-Si-X samples. As compared with Al-25SiCuMg (IT) alloys, Al-25SiCuMg (PT) alloys in both as thixocast and T6 condition show obvious improvement in hardness and UTS, but decline in ductility behavior. The strength improvement is clearly derived from the drastic refinement in microstructure on Al-25SiCuMg (PT) (Fig.3a) compared with Al-25SiCuMg (IT) (Fig.4b). However, the low ductility observed is contrary to our expectation. This low ductility is suggested due to clustering of primary Si particulates after thixocasting in Al-25SiCuMg alloys (Fig.3a), since fracture tends to initiate from or propagate through the Si particulate agglomerates [11]. According to this reason, as Al-20SiFe (PT) shows less extent of Si clustering (Fig.3b), it exhibits slightly higher ductility than Al-25SiCuMg alloys.

The UTS values obtained on the powder thixocast alloys are close to those obtained by P. J. Ward [12], 200-300 MPa, who thixocast the hypereutectic Al-Si-X alloys using feedstock made by spray forming followed by extrusion. This indicates that the powders were consolidated after powder thixocasting.

*3.3 Wear performance*

Figure 5 shows the wear rate varied with load obtained on the thixocast alloys. It is worthy to note that the wear behavior of Al-25SiCuMg (PT) alloys apparently fall into three regions, regions I-III as depicted in Fig.5a and b. At the lowest level of load (region I) the wear rate increases almost linearly with load. When load further increases beyond a critical value, the wear rate begins to decrease with load (region II). This is followed by an increase in wear rate with load until specimen seizure happens (region III).

Figure 5 shows that at the lowest level of load all alloys exhibit similar wearing behavior in region I, i.e. wear rate increases linearly with load. However, the behavior in regions II and III shows distinct difference among the alloys. Al-25SiCuMg (PT) and Al-20SiFe (PT) alloys exhibit clear profiles of the regions II and III, but Al-25SiCuMg (IT) and LM13 alloys display the profile ambiguously. Owing to the presence of the distinct region II and III, Al-25SiCuMg (PT) and Al-20SiFe (PT) alloys present their superior performance in heavy-load wearing condition, as compared with Al-25SiCuMg (IT) and LM13 alloy.

Indeed, this three-region wear behavior, in particular the obvious decreasing wear rate with load as shown in region II, obtained on powder thixocast

Al-25SiCuMg (PT) alloy was seldom reported in prior literatures. It has been recognized that when slide against an iron-based counterface, Al-Si alloys usually show mild wear, severe wear and seizure regimes over range of applied contact load [13]. The mild wear regime, under which wear rate increases proportionally with load, can be corresponding to the region I observed here, as is revealed in Fig.5. However, the sever wear regime, under which wear rate increases with load about exponentially, is distinct from the regions II and III observed here.

In Fig.5, however, we find that owing to the presence of region II the powder thixocasting alloys, Al-25SiCuMg (PT) and Al-20SiFe (PT), possess wonderful wearing performance under high load wearing conditions compared with LM13 and Al-25SiCuMg (IT). Inspecting the wear surface of the powder thixocast specimens in the regions II, we found a mechanical mixing layer (MML) [14] comprised of small particulates of Fe, $Al_2O_3$, Si embedded uniformly in a severely deformed Al matrix. It is suggested that the evolution of MML causes change of the wear rate from regions II to III as shown in Fig.5. But, further investigation is necessary to elucidate it.

Archard [15] proposed a model to explain the wear rate behavior in mild wear regime, i.e. region I in Fig.5. He suggested that when two sliding surfaces contact together, the applied load is carried by the asperities of the contacting surfaces. On sliding, the asperities are worn away because adhesion occurs, meanwhile new asperities form to alternatively carry the applied load. And, based on this, Archard proposed a volume of wear W after a certain sliding distance d is given by: W/d=(KL)/(3H), where K is a constant, L is the normal applied force and H the penetration hardness of the surface being worn away. This model predicts that the harder material the better wear performance. This is consistent with the truth observed on Al-25SiCuMg (PT) alloy in both as thixocast and T6 conditions. Since it has the highest hardness among the alloys listed in Table 2, it shows the best wear performance in Fig.5. However, this is not consistent with the results when comparing Al-25SiCuMg (IT) with LM13 in T6 condition (Fig.5b). Although the former has higher hardness, it possesses lower wear performance than the latter. Large primary Si particulates in the former alloy should be responsible for this exception, since fragile Si particulates are easily fractured and worn away during wearing.

Beside the low wear rate mentioned, another feature of wear performance obtained on the powder thixocast alloys is their high seizure stress (Fig.5). Due to the role of primary Si particulates as an anti-seizure agent [13], it has been recognized that in Al-Si alloys the higher Si contents the higher seizure resistance. This is the reason why hypereutectic Al-25SiCuMg and Al-20SiFe alloys show higher seizure resistance than eutectic LM13 alloy. However, comparing with Al-25SiCuMg (IT) alloy, the Al-25SiCuMg (PT) alloy still shows higher seizure stress in T6 condition (Fig.5b). This high seizure resistance obtained may also be associated with the refinement of primary Si using powder thixocasting technique.

*3.4 High temperature compression strength*

Figure 6 shows the compressive strength obtained on the experimental alloys at temperature from 25°C to 400°C. The materials in performance are Al-25SiCuMg (PT)> Al-25SiCuMg (IT)>LM13>Al-20SiFe (PT). This is similar to the ranking obtained on hardness values of these alloys (Table 2). A previous study [10] proposed that element Fe improve the elevated mechanical properties through the precipitation of intermetallic phases, such as δ-$Al_4FeSi_2$ and β-$Al_5FeSi$ that are relatively stable at temperature of up to 300°C. However, it is found that the Al-20SiFe (PT) alloy shows the worse compressive strength here. This may be due to the excessive grain coarsening of the intermetallic precipitates during semisolid processing as described above. Although the Al-20SiFe (PT) alloy shows poor compressive strength at elevated temperature, it also possesses superior wear resistance in high loading condition compared with Al-25SiCuMg (IT) and LM13 alloys (Fig.5a). This suggests that wear loss under heavy load on Al-Si-X alloys is not related to their compressive strength at elevated temperatures.

## 4. CONCLUSIONS

1. This study has demonstrated the feasibility of the new approach - powder thixocasting to achieve near-net shape forming of hypereutectic Al-Si-X alloys with fine microstructure as well as high wear performance.
2.In the powder thixocast alloys Al-20Si-5Fe and Al-25Si-2.5Cu-1Mg, the variation of wear rate with applied load clearly falls three regions.
3. In the alloys LM13 and Al-25Si-2.5Cu-1Mg fabricated using conventional liquidus casting routes, the variation of wear rate with load exhibit clearly only the region I but exhibit ambiguously the region II and III.
4. The powder thixocast alloys perform wear resistance much better than the conventional alloys LM13 and Al-25Si-2.5Cu-1Mg under heavy load condition or in T6 conditions.

## ACKNOWLEDGEMENTS

The authors would like to thank the National Science Council of the Republic of China for financially supporting this research under Contract No. NSC 91-2216-E-009-022.

## REFERENCES

1. J.E. Hatch, *Aluminum: Properties and Physical Metallurgy* (ASM: Metals Park, Ohio 1984) pp. 346-347.
2. J.E. Gruzleski and B.M. Closset, *The Treatment of Liquid Aluminum-Silicon Alloys* (AFS: Des Plaines, Illinos 1990) pp. 107-126.
3. Kiyoaki Akechi, 1989, US Patent 4,838,936.
4. H.So, W.C.Li and H.K.Hsieh, *J. Mat. Process. Technol*, 2001, **114**, 18-21.
5. C.M. Chen, C.C. Yang and C.G. Chao, *Mater. Sci. Eng.* A366 (2004) 183-194.
6. J.E. Hatch, *Aluminum: Properties and Physical Metallurgy*, (ASM: Metals Park, Ohio, 1984), pp.49.
7. L.F. Mondolfo, *Aluminum Alloys: Structure and Properties* (Butter Worths: Mass., Boston, 1976), pp.645.
8. Y.S. Choi, J.S. Lee, W.T. Kim and H.Y. Ra, *J. Mater. Sci.* 34, 1999, 2163-2168.
9. F. Wang, B. Yang, X.J.Duan, B.Q. Xiong, J.S.Zhang, *J. Mater. Process. Technol.* 137,2003, 191-194.
10. V.C. Srivastava, P. Ghosal, and S.N. Ojha., *Mater. Lett.* 56, 2002, 797-801.
11. M.C. Flemings, *Metall. Trans. A* 1991, **22**, 957-981.
12. P.J. Wars, H.V. Atkinson, P.R.G. Anderson, L.G.

Elias, B. Garcia, L. Kahlen, and J-M. Rodriguez-Ibabe, *Acta mater.* 1996, **44 (5)**, 1717-1727.
13. A. Somi Reddy, B.N. Pramila Bai, K.S.S. Murthy and S.K. Biswas, *Wear*, 1994, **171**, 115-127.
14. X.Y. Li and K.N. Tandon, *Wear*, 1999, **225-229**, 640-648.
15. Archard, J.F., J. Appl. Phys., 1953, 24, 981-988.

Table 1. Chemical compositions of the alloys

| Alloy | Processing route | Chemical composition (wt%) | | | | | | | |
|---|---|---|---|---|---|---|---|---|---|
| | | Si | Cu | Mg | Mn | Fe | Ni | Ti | Al |
| Al-25SiCuMg (PT) | Powder thixocast | 24.6 | 2.56 | 1.04 | 0.47 | 0.16 | 0.01 | 0.03 | Bal. |
| Al-20SiFe (PT) | Powder thixocast | 20.0 | 0.02 | 0.02 | 0.01 | 5.64 | — | — | Bal |
| Al-25SiCuMg (IT) | Ingot thixocast | 24.2 | 2.25 | 1.08 | 0.08 | 0.69 | 0.04 | 0.08 | Bal |
| LM13 | Ingot metallurgy | 11.6 | 1.08 | 1.12 | 0.01 | 0.50 | 1.00 | 0.03 | Bal |

Table 2. Strength and Hardness of the alloys

| Alloy | Heat treatment | UTS (Mpa) | Elongation (%) | Hardness (Hv, 100gf) |
|---|---|---|---|---|
| Al-25SiCuMg (PT) | As thixocast | 224 | 0.20 | 144 |
| | T6 | 304 | 0.12 | 175 |
| Al-25SiCuMg (IT) | As thixocast | 205 | 0.35 | 108 |
| | T6 | 254 | 0.28 | 152 |
| Al-20Si5Fe (PT) | As thixocast | 192 | 0.48 | 82 |
| LM13 | As cast | 245 | 1.8 | 86 |
| | T6 | 330 | 1.5 | 143 |

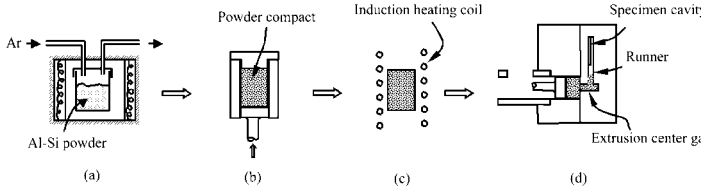


Fig.1 Schematic diagram of the powder thixocasting procedures

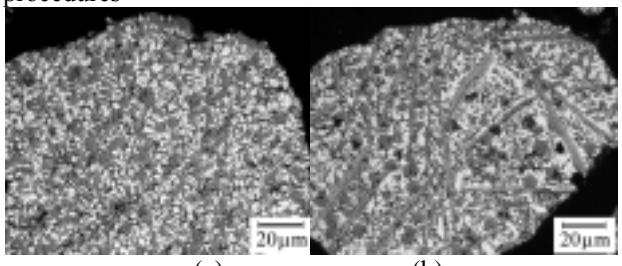


(a) (b)

Fig.2 Typical optical micrographs of gas-atomized (a) Al-25SiCuMg (b) Al-20SiFe powders.

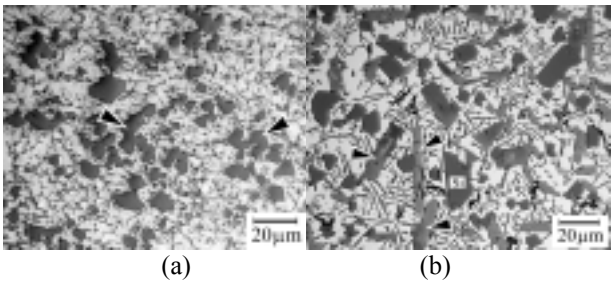


(a) (b)

Fig.3 Typical optical micrographs of the thixocast samples (a) Al-25SiCuMg (PT), arrows indicate clustering of primary Si after thixocasting, and (b) Al-20SiFe (PT), arrows indicate β - Al5SiFe phase.

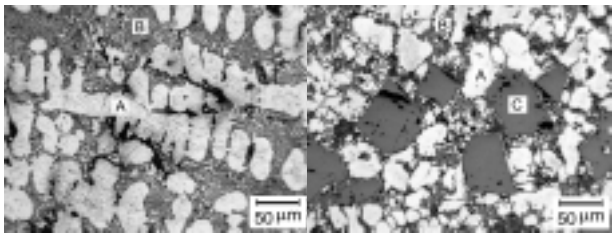


(a) (b)

Fig.4 Typical optical micrographs of (a) the Al-25SiCuMg feedstock fabricated by liqudus casting and (b) the Al-25SiCuMg (IT) alloy after thixocasting.

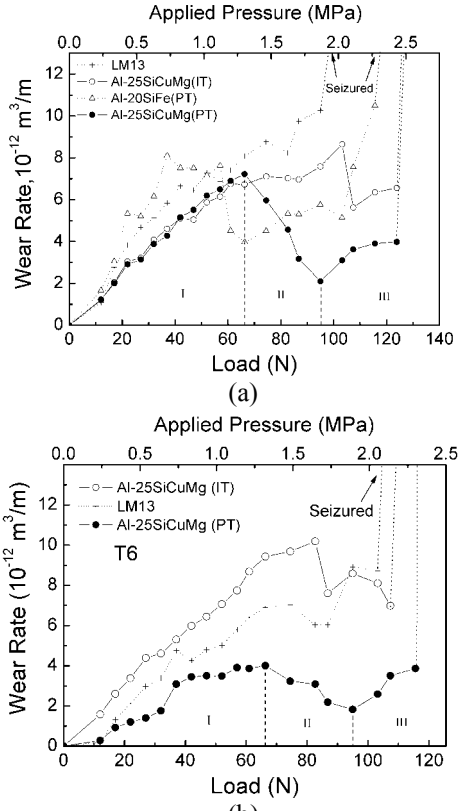


Fig.5 Wear rate variation with applied load obtained on thixocast hypereutectic Al-Si-X alloys at (a) as thixocast (b) T6 states. The Al-25SiCuMg (PT) alloys (●) show obviously three-region wear behavior.

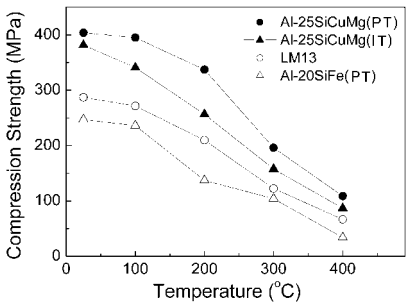


Fig.6 High temperature compression strength of Al-Si-X thixocast alloys, commercial LM13 alloy is also shown for comparison.